Effect of phase transformations on the shape of the unloading curve in the nanoindentation of silicon

Vladislav Domnich and Yury Gogotsi[a)]
Department of Mechanical Engineering, University of Illinois at Chicago, Chicago, Illinois 60607-7022

Sergey Dub
Institute for Superhard Materials, Kiev 254074, Ukraine

(Received 1 December 1999; accepted for publication 21 February 2000)

Silicon wafers subject to depth-sensing indentation tests have been studied using Raman microspectroscopy. We report a strong correlation between the shape of the load-displacement curve and the phase transformations occurring within a nanoindentation. The results of Raman microanalysis of nanoindentations in silicon suggest that sudden volume change in the unloading part of the load-displacement curve (''pop-out'' or ''kink-back'' effect) corresponds to the formation of Si–XII and Si–III phases, whereas the gradual slope change of the unloading curve (''elbow'') is due to the amorphization of silicon on pressure release. The transformation pressures obtained in nanoindentation tests are in agreement with the results of high pressure cell experiments.
© *2000 American Institute of Physics.* [S0003-6951(00)02916-8]

Response of silicon to depth-sensing indentation has received extensive attention during the past decade.[1–6] Unlike other similar materials, silicon often shows a characteristic ''kink-back'' or ''pop-out'' during indentation, which reveals itself as a step in the unloading part of the load-displacement curve.[4,7] An attempt to attribute the pop-out to the formation of a deep lateral crack beneath the indenter resulting in an uplift of the surrounding surface[2] found no evidence in the transmission electron microscopy studies.[7] The pop-out can also be explained by a phase transformation that occurs beneath the indenter and is accompanied by a sudden volume release. It is well known that silicon transforms from the cubic diamond phase (cd or Si–I) to a metallic phase with the β-tin structure (Si–II) at elevated pressures.[8–10] On pressure release, amorphous silicon or several metastable phases can be formed from Si–II depending on experimental conditions. The metastable phases include the body centered cubic phase (bc8 or Si–III) and its rhombohedral distortion (r8 or Si–XII),[11] hexagonal diamond phase (hd or Si–IV),[12] and two simple tetragonal phases (Si–VIII and Si–IX).[13] Conductivity measurements[14] confirmed the metallization of silicon during nanoindentation, while scanning[1] and transmission electron microscopy[15] revealed amorphous silicon and plastically extruded material around the indentations. Our recent work demonstrated that Raman microspectroscopy could be successfully used for phase analysis of nanoindentations and confirmed phase transformation of Si during nanoindentation tests.[16] However, specific features of the unloading curves (pop-outs or elbows) have not been assigned to particular transformation processes yet.

In this letter, we report the results of the Raman microspectroscopy analysis of nanoindentations made on polished (111) and etched (100) Si wafers. Two depth-sensing indentation devices were used, NanoIndenter®II in Kiev and NanoIndenter®XP (MTS) in Chicago, to obtain reproducible and system-independent results. Nanoindentation tests were performed using a Berkovich pyramid in the following way: loading to 30–50 mN and unloading by 90%, holding for 20 s at 10% of the maximum load for thermal drift measurements, and complete unloading. The loading rates ranged from 1 to 3 mN/s. The same rates were used for loading and unloading. The choice of such experimental parameters was imposed by the fact that under these conditions, the probability of observing either a pop-out or an elbow in the unloading curve is almost the same. The transformation pressures were calculated from the load-displacement data as average contact pressures following the procedure of Ref. 17.

Raman spectra were acquired in backscattering geometry using a Ramascope 2000 (Renishaw, UK) Raman microspectrometer. The scattered light from an Ar^+ laser (excitation wavelength 514.5 nm) was dispersed with a diffraction grating and then detected with a charge coupled device. Due to virtually the same size of nanoindentations and a laser spot (~ 1 μm), only some average vibrational response from within the indentations was recorded, including a small contribution from the pristine region of the silicon wafer unaffected by the indenter.

In total, 60 nanoindentations have been made in each sample using the same experimental parameters. Three typical load-displacement curves obtained in the experiments are shown in Fig. 1. Normally, slower loading/unloading rates (1 mN/s) and higher maximum loads (50 mN) lead to the appearance of pop-outs in the unloading curves [Fig. 1(a)], while at faster rates (3 mN/s) and lower loads (30 mN), elbows were more often observed [Fig. 1(c)]. Also, several indentations showed a mixed response, when the change in slope of the unloading curve was followed by a sudden decrease in indentation depth [Fig. 1(b)]. This tendency remained essentially the same for different devices used (NanoIndenter®II or NanoIndenter®XP) and did not depend on the crystallographic orientation and surface finish of the

a)Author to whom correspondence should be addressed; electronic mail: ygogotsi@uic.edu

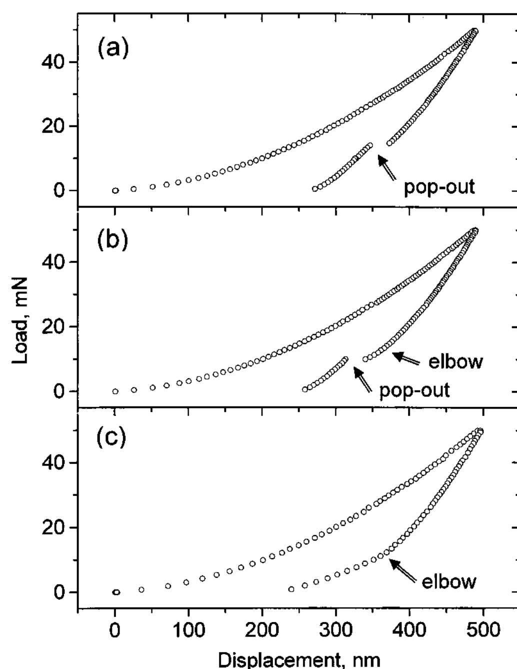

FIG. 1. Three types of load-displacement curves in the nanoindentation of Si, obtained at the loading rate of 3 mN/s and maximum load of 50 mN.

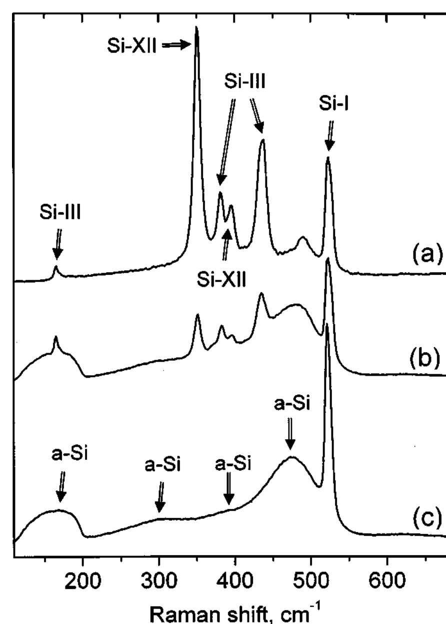

FIG. 2. Three types of Raman spectra from nanoindentations in Si, revealing metastable phases (a), amorphous Si (c), and a mixture of *a*-Si, Si–III and Si–XII (b).

samples [(111) polished or (100) etched wafers]. The latter fact implies that in the nanoindentation experiments, the response of silicon on pressure release is affected mostly by its transformation (metallization) during the loading cycle, and to a lesser extent by the state of the wafer surface prior to indentation.

Raman spectra of all indentations made using NanoIndenter®XP were taken immediately after the test. With the samples indented using NanoIndenter®II, 2 months passed between the depth-sensing test itself and the Raman microspectroscopy studies of the sample sent to the U.S. from Ukraine. In both cases, three characteristic types of spectra were observed (Fig. 2). The spectrum in Fig. 2(a) shows a typical Raman response of Si–III and Si–XII phases.[18–21] It matches almost exactly the Raman spectra obtained from some areas within microindentations in silicon,[21,22] with the exception of a rather strong band at 520 cm^{-1} corresponding to the Si–I phase (pristine silicon) and present in the Raman spectrum for reasons discussed above. In the literature, bands at 166, 382, and 433 cm^{-1} have been assigned to the Si–III phase, while the bands at 350 and 394 cm^{-1} can serve as a fingerprint of the Si–XII phase.[19,21] The origin of the peak at 490 cm^{-1} has not yet been unambiguously identified.

Another typical Raman spectrum from nanoindentations is presented in Fig. 2(c). The same response has been obtained from the amorphized areas within microindentations in silicon.[21,22] Broad peaks around 170, 300, 390, and 470 cm^{-1} have been identified as transverse acoustic-like, longitudinal acoustic-like, longitudinal optical-like and transverse optical-like bands of amorphous silicon, respectively,[23] while a peak at 520 cm^{-1} represents the pristine Si–I as before. Finally, the Raman spectra of several nanoindentations revealed traces of both amorphous silicon and metastable Si–III and Si–XII phases [Fig. 2(b)].

For an adequate data representation, we compared load-displacement curves and corresponding Raman spectra of 120 nanoindentations made using two different depth-sensing indentation devices (NanoIndenter®II and NanoIndenter®XP) in two different types of samples [(111) polished and (100) etched Si wafers]. Table I summarizes the results. In 93% of cases, Raman spectra showing metastable phases [Fig. 2(a)] were obtained from the nanoindentations with a pop-out in the load-displacement curve [Fig. 1(a)]. In 95% of cases, Raman spectra of amorphous silicon [Fig. 2(c)] corresponded to the nanoindentations with a change in slope (elbow) of the unloading curve [Fig. 1(c)]. The Raman spectra showed traces of both amorphous silicon and metastable Si–III and Si–XII phases [Fig. 2(b)] when the indentation curves revealed both elbow and pop-out events [Fig. 1(b)].

The results obtained suggest a strong correlation between the shape of the unloading curve and the structural changes occurring in silicon during nanoindentation experiments. The pop-out effect is a consequence of an abrupt phase transformation from metallic Si–II to either Si–III or Si–XII, accompanied by a sudden volume increase and hence the uplift of the material surrounding an indenter. From theoretical analysis and pressure cell experiments, Si–XII is supposed to form first in the pressure of the pop-out, with a subsequent slow, but never complete transformation to Si–III during unloading.[11,20,21] The elbow in the unloading

TABLE I. Number of nanoindentations showing specific behavior during the depth-sensing indentation test.

Phases observed in the Raman spectrum	Number of the unloading curves showing		
	Pop-out	Elbow and pop-out	Elbow
Si–III, Si–XII	53	3	1
Si–III, Si–XII, *a*-Si	1	19	1
a-Si	0	2	40

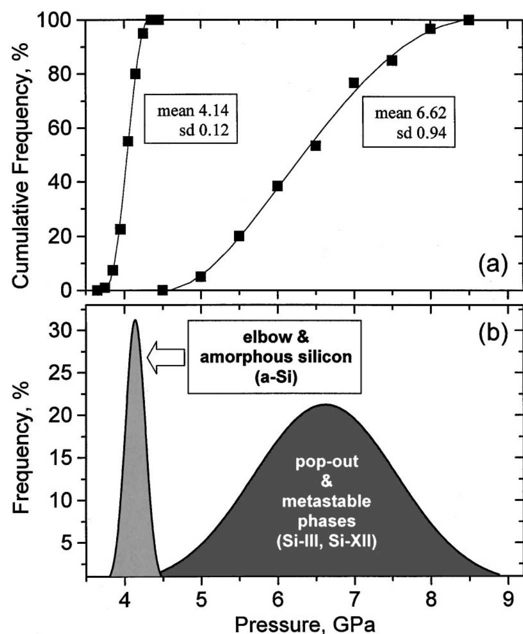

FIG. 3. Statistical analysis of the results of Raman microspectroscopy of nanoindentations. Continuous cumulative distributions (a) and estimated probability density functions (b). The curves represent a probability of formation of either metastable phases or amorphous silicon during unloading vs average contact pressure. The mixture of *a*-Si, Si–II, and Si–XII is observed between the two curves (4.5–5.5 GPa).

curve of the indentation diagram corresponds to the formation of an amorphous phase of silicon. The gradual change in slope of the unloading curve in this case is the result of the material's expansion during slow transformation from metallic to the amorphous semiconducting phase, which contributes to the indenter uplift.

We have presented the results for all nanoindentation tests schematically in Fig. 3. Phase transformation from Si–II to a metastable crystalline state takes place in the pressure range of 5.0–8.5 GPa, with the mean value of 6.62 GPa. This is in reasonable agreement with high pressure cells experimental values of 8–10 GPa.[11,24] The discrepancy could be attributed to the fact that the average contact pressure beneath the indenter is determined by both deviatoric and hydrostatic components of stress. As suggested by Gilman,[25] phase transformations during indentation may be induced by shear (bond bending) rather than compression (bond shortening), thus one would expect lower numbers of transition pressures obtained from indentation experiments as compared to purely hydrostatic conditions in diamond anvil studies.

At pressures less than 4.5 GPa, only amorphous silicon is being formed (Fig. 3). In the range of 4.5–5.5 GPa, both partial amorphization and phase transformation of metallic silicon to metastable phases can take place. Broad variation in the pressure of the reverse phase transformation of Si from the metallic phase reflects the statistical nature of the process, which is related to the release of elastic energy accumulated in the indented material.

This research was supported by the National Science Foundation, Grant No. DMR-9874955.

[1] G. M. Pharr, W. C. Oliver, and D. S. Harding, J. Mater. Res. **6**, 1129 (1991).
[2] G. M. Pharr, Mater. Res. Soc. Symp. Proc. **239**, 301 (1992).
[3] E. R. Weppelmann, J. S. Field, and M. V. Swain, J. Mater. Res. **8**, 830 (1993).
[4] S. V. Hainsworth, A. J. Whitehead, and T. F. Page, in *Plastic Deformation of Ceramics*, edited by R. C. Bradt, C. A. Brookes, and J. L. Routbort (Plenum, New York, 1995), pp. 173–184.
[5] T. Suzuki and T. Ohmura, Philos. Mag. A **74**, 1073 (1996).
[6] J. S. Williams, Y. Chen, J. Wong-Leung, A. Kerr, and M. V. Swain, J. Mater. Res. **14**, 2338 (1999).
[7] T. F. Page, W. C. Oliver, and C. J. McHargue, J. Mater. Res. **7**, 450 (1992).
[8] S. Minomura and H. G. Drickamer, J. Phys. Chem. Solids **23**, 451 (1962).
[9] M. C. Gupta and A. L. Ruoff, J. Appl. Phys. **51**, 1072 (1980).
[10] J. Z. Hu and I. L. Spain, Solid State Commun. **51**, 263 (1984).
[11] J. Crain, G. J. Ackland, J. R. Maclean, R. O. Piltz, P. D. Hatton, and G. S. Pawley, Phys. Rev. B **50**, 13043 (1994).
[12] G. Weill, J. L. Mansot, G. Sagon, C. Carlone, and J. M. Besson, Semicond. Sci. Technol. **4**, 280 (1989).
[13] X. S. Zhao, F. Buehler, J. R. Sites, and I. L. Spain, Solid State Commun. **59**, 678 (1986).
[14] G. M. Pharr, W. C. Oliver, R. F. Cook, P. D. Kirchner, M. C. Kroll, T. R. Dinger, and D. R. Clarke, J. Mater. Res. **7**, 961 (1992).
[15] D. L. Callahan and J. C. Morris, J. Mater. Res. **7**, 1614 (1992).
[16] Y. G. Gogotsi, V. Domnich, S. N. Dub, A. Kailer, and K. G. Nickel, J. Mater. Res. **15** (in press).
[17] N. V. Norikov, S. N. Dub, Yu. V. Milman, I. V. Gridnera, and S. I. Chugunova, J. Superhard Materials No. 3, 32 (1996).
[18] R. J. Kobliska, S. A. Solin, M. Selders, R. K. Chang, R. Alben, M. F. Thorpe, and D. Weaire, Phys. Rev. Lett. **29**, 725 (1972).
[19] M. Hanfland and K. Syassen, High Press. Res. **3**, 242 (1990).
[20] R. O. Piltz, J. R. Maclean, S. J. Clark, G. J. Ackland, P. D. Hatton, and J. Crain, Phys. Rev. B **52**, 4072 (1995).
[21] A. Kailer, Y. G. Gogotsi, and K. G. Nickel, J. Appl. Phys. **81**, 3057 (1997).
[22] G. Lucazeau and L. Abello, J. Mater. Res. **12**, 2262 (1997).
[23] M. Marinov and N. Zotov, Phys. Rev. B **55**, 2939 (1997).
[24] J. Z. Hu, L. D. Merkle, C. S. Menoni, and I. L. Spain, Phys. Rev. B **34**, 4679 (1986).
[25] J. J. Gilman, Mater. Res. Soc. Symp. Proc. **276**, 191 (1992).